Mixed stack organic semiconductors: The anomalous case of the BTBT-TCNQFx series

Mixed stack organic semiconductors:

The anomalous case of the BTBT-TCNQF$_x$ series

Nicola Castagnetti[§], *Alberto Girlando*[§]*, *Matteo Masino*[§], *Corrado Rizzoli*[§]*, *Concepció Rovira*[¶]

[§] Dipartimento di Scienze Chimiche, della Vita e della Sostenibilità Ambientale (SCVSA) and INSTM-UdR Parma, Università di Parma, Parco Area delle Scienze 17/a, IT-43124 Parma, Italy

[¶] Department of Molecular Nanoscience and Organic Materials, Institut de Ciència de Materials de Barcelona (ICMAB-CSIC) and Networking Research Center on Bioengineering, Biomaterials and Nanomedicine (CIBER-BBN), ES-08193 Bellaterra, Spain

ABSTRACT We present a detailed structural and spectroscopic characterization of three mixed stack organic semiconductors, where benzothieno-benzothiophene electron Donor is associated with Fluorine-substituted TCNQ of increasing electron affinity. BTBT-TCNQ and BTBT-TCNQF$_2$ are isomorphous, whereas the three-dimensional packing of BTBT-TCNQF$_4$ is different. Rather surprisingly, we found that the degree of charge transfer is almost constant along the series, at variance with what has been found in analogous co-crystal series in which TCNQF$_x$ are involved. We explain this finding in terms of the Madelung energy resulting from inter-stack packing of the co-crystals, and of the fact that both the HOMO and HOMO-1 of BTBT are involved in the CT mechanism. We also propose that the difference in inter-stack packing resulting from increasing F substitution is a consequence of electrostatic interactions.

INTRODUCTION

In the quest of new and more efficient organic semiconductors for low-cost, eco-friendly electronic devices, considerable attention has been recently devoted to two-component, mixed stack charge transfer (CT) crystals, due to the suggestion of possible ambipolar transport[1] and of facile tuning of the band gap by changing one of the two components, generally the electron acceptor, applying the so-called molecular electrical doping.[2–5] Benzothieno-benzothiophene (BTBT) alkylated derivatives that shown outstanding *p*-channel semiconducting properties[6,7] have recently been combined with $TCNQF_x$ acceptors to explore the possibilities of the two-component approach.[8,9] Surprisingly enough, the obtained transistors are of *n*-type,[9,10] and the degree of charge transfer do not correlate with the $TCNQF_x$ acceptor strength, like it happens for instance with other mixed stack CT crystals, e.g. the perylene-$TCNQF_x$ series.[3,4]

In order to disentangle the possible effects of the alkyl side-chains on this behavior, we decided to investigate the physical properties of the charge transfer crystals of the $TCNQF_x$ series of acceptors (x= 0, 2, 4) with unsubstituted BTBT. Independently from us, the same crystals were prepared by Sato *et al.*,[11] and studied in OTFT devices. Here we shall focus on a more detailed characterization, accompanied by a theoretical analysis aimed at understanding the peculiar properties of this series of crystals.

EXPERIMENTAL SECTION

Sample preparation

TCNQ, $TCNQF_2$ and $TCNQF_4$ (purity ≥ 98%) were purchased from TCI. BTBT (purity ≥ 99,99 %) was purchased from Laboratoire de Chimie des Polymers (Université Libre de Bruxelles). Each material was utilized as received. For the growth of single crystals, 2 mg of BTBT were dissolved in dichlorobenzene (DCB) with the proper amount of $TCNQF_x$ to form an equimolar solution. The solutions were heated up to 90°C and the total volume of DCB was determined to have saturated starting solutions. Each solution was then inserted in a programmable oven that was set up to decrease the temperature from 90 to 24°C in 48h. The slow and controlled cooling process provided a way to reach the supersaturation conditions in a less dramatic way than the simple spontaneous cooling of the solution at room temperature, thus enabling the formation of diffraction quality single crystals. Finally the so obtained crystals were carefully extracted and dried on filter paper.

X-ray diffraction measurements

Single crystals of the three complexes were mounted on a Bruker SMART 1000 CCD diffractometer equipped with graphite monochromated Mo Kα radiation (λ = 0.71073 Å) fine-focus sealed tube. The intensity data were collected using ω scan at 294(2) K. Cell refinements and data reductions were performed using the Bruker SAINT software.[12] Multi-scan absorption corrections were applied empirically to the intensity values (T_{min} and T_{max} = 0.954, 0.992 for BTBT-TCNQ; 0.965, 0.994 for BTBT-$TCNQF_2$; 0.918, 0.982 for BTBT-$TCNQF_4$) using SADABS.[12] The structures were solved by direct methods using the program SHELXT[13] and refined with full-matrix least-squares based on F^2 using the program SHELXL2014/7.[14] All non-hydrogen atoms were refined anisotropically. Hydrogen atoms were placed geometrically and

refined using a riding model approximation, with C–H = 0.93 Å and with U_{iso}(H) = 1.2 U_{eq}(C). The molecular graphics were prepared using the ORTEP,[15] SCHAKAL99,[16] and Jmol[17] programs.

Spectroscopic measurements

Infrared (IR) spectra of the crystals were recorded with a Bruker IFS66 Fourier transform IR (FT-IR) spectrometer coupled to an IR microscope Hyperion 1000. Spectral resolution: 2 cm^{-1}. The Raman spectra were recorded with a Renishaw 1000 Raman spectrometer equipped with the appropriate edge filter, and coupled to a Leica M microscope. A Lexel Kr laser was used as light source. Samples of BTBT-TCNQF_2 and BTBT-TCNQF_4 were excited with the 676-nm line, while samples of BTBT-TCNQ were excited with the 532 nm line.

Theoretical calculations

We have followed the approach recently developed by some of us.[18,19] The method uses ground-state Density Functional (DFT) calculations (Gaussian09 package[20]) for individual molecules and Donor-Acceptor (DA) dimers, and on the atomistic modeling of intermolecular electrostatic interactions. All calculations have been performed in vacuum using the unrestricted ωB97XD hybrid functional together with the 6-31+G* basis set. The average charge residing on BTBT and TCNQF_x molecules is estimated on the basis of the computed Hirshfeld atomic charges. Intermolecular charge transfer integrals have been calculated by using ADF[21] with TZP basis and GGA:PBE functional. The electrostatic interaction V within a DA pair and the Madelung energy M are computed by adopting the point-charge approximation of the molecular charge density based on ESP atomic charges computed for neutral and charged molecules and lattices. The crystal electrostatic sums have been obtained for finite clusters of increasing size using the MESCAL code.[18]

RESULTS

All compounds crystallize as alternating D-A stacks. The basic structural parameters and information useful to the presentation of the results are reported in Table 1. Full information is given in the Supporting Information and in the deposited CIF files (CCDC: 1556355, 1556356, 1556357). The structures coincide with those independently reported by Sato *et al.*[11]

Table 1. Room temperature (294 K) crystal structures of BTBT-TCNQ, BTBT-TCNQF$_2$ and BTBT-TCNQF$_4$.

	BTBT-TCNQ	BTBT-TCNQF$_2$	BTBT-TCNQF$_4$
Space group	*P*-1	*P*-1	$P2_1/c$
Z	1	1	2
T/ K	294(2)	294(2)	294(2)
a /Å	7.211(3)	7.1628(12)	7.961(2)
b /Å	8.009(4)	7.9475(13)	7.0803(19)
c /Å	8.999(4)	9.1113(15)	19.113(5)
α (deg)	81.261(6)	80.918(2)	90
β (deg)	89.379(6)	89.573(2)	99.347(5)
γ (deg)	87.664(4)	87.924(2)	90
V /Å^3	513.3(4)	511.83(15)	1063.0(5)
DA interplanar distance /Å	3.3862(8)	3.3495(5)	3.3004(4)
DA interplanar dihedral angle /°	3.80(6)	2.01(6)	0.5(2)

BTBT-TCNQ and BTBT-TCNQF$_2$ are isomorphous, both belonging to the triclinic P-1 space group. The molecules are stacked along the *a* crystal axis, and there is one DA pair per unit cell. Notice that the β angle is almost 90°. BTBT-TCNQF$_4$ instead crystallizes in the monoclinic $P2_1/c$ group, with two DA pairs per unit cell, stacked along the *b* crystal axis. In BTBT-TCNQF$_4$ the volume per DA pair is appreciably larger (531.5 Å^3) than in the other two CT crystals. Figure 1 puts in evidence the similarity in the stack structure of the isomorphous BTBT-TCNQ and

BTBT-TCNQF$_2$, and of BTBT-TCNQF$_4$.. In all cases the molecules are inclined by approximately the same angle with respect to the stacking axis. However, the reciprocal arrangement of the stacks is different: The layers perpendicular to the stacking axis are made up of equal molecules in BTBT-TCNQ and BTBT-TCNQF$_2$ (Figures 1 and S4, S5), whereas they are arranged in a chessboard layout in BTBT-TCNQF$_4$ (Figures 1 and S6).

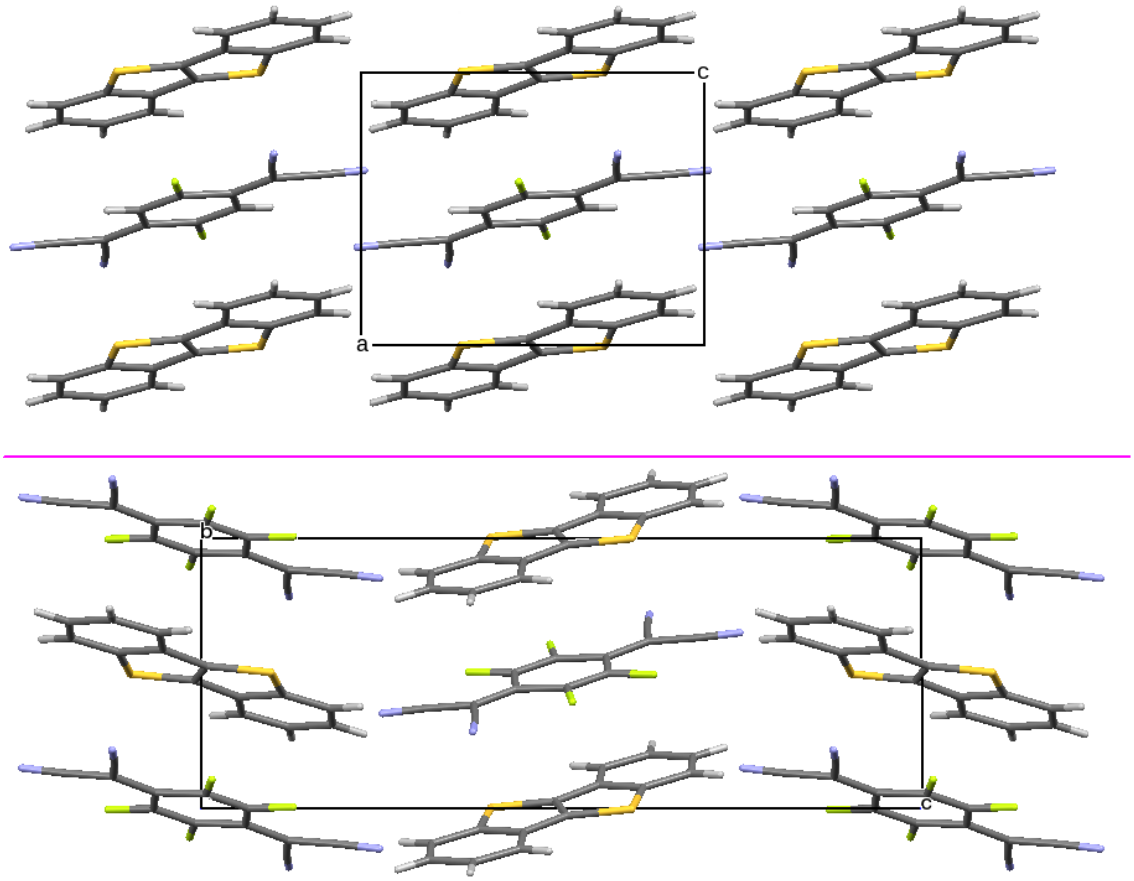

Figure 1. (Top) Crystal structure of BTBT-TCNQF$_2$ viewed from the *b* axis. (Bottom) Crystal structure of BTBT-TCNQF$_4$ viewed from the *a* axis. The chosen view puts in evidence the stack structure and the three dimensional stack arrangment.

The average planes of BTBT and TCNQF$_x$ are slightly inclined each other, and the inclination decreases in going from TCNQ to TCNQF$_4$, as the inter-planar distance does. The same trend,

albeit less pronounced, is found in the analogous series of (diC_8-BTBT)-$TCNQF_x$.[9] Of course, the reciprocal arrangement of D and A molecules is such to give the optimum CT overlap. However, in the case of BTBT complexes the overlap is not only between the HOMO and LUMO of the DA pair, but also involves the HOMO-1 orbital of BTBT.[8,9] This is pictorially shown in Figure 2, where the HOMO, HOMO-1 of BTBT and the LUMO of TCNQ are drawn together with the projection of BTBT molecule over $TCNQF_2$ (the projection over TCNQ and $TCNQF_4$ is similar). We also notice that at variance with other complexes of $TCNQF_2$, for instance with perylene,[4] in BTBT-$TCNQF_2$ there is no disorder in the F atoms position resulting from rotational disorder, due to the asymmetrical superposition of BTBT and $TCNQF_2$ along the stack (bottom left side of Figure 2).

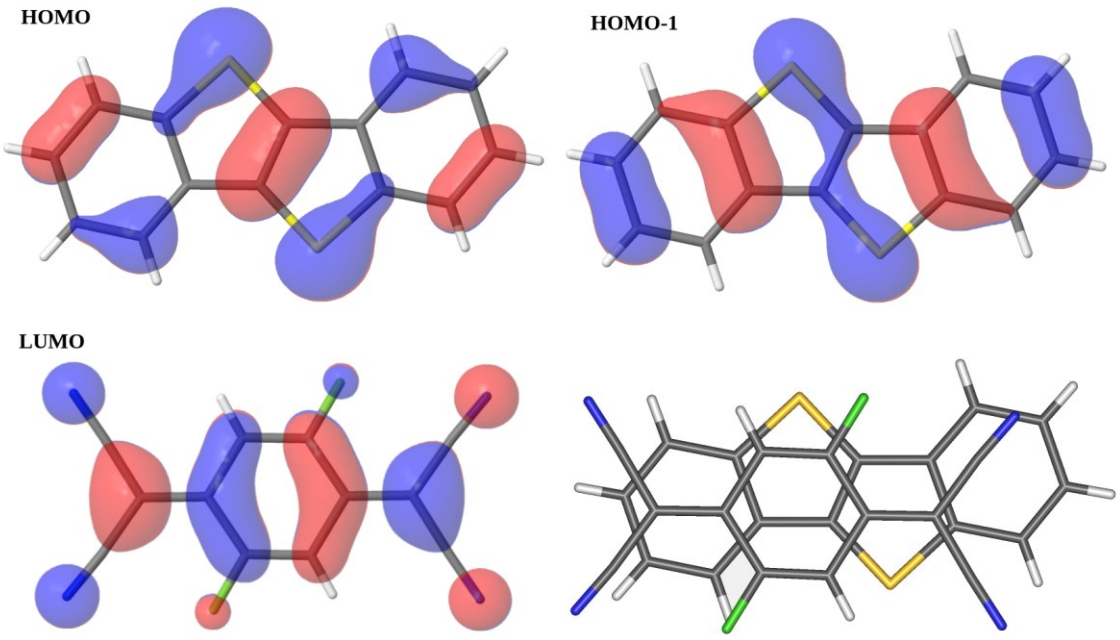

Figure 2. Pictorial representation of the HOMO, HOMO-1 of BTBT and of LUMO of TCNQF2, and projection of $TCNQF_2$ on BTBT plane along the stacking axis.

We now turn attention to the determination of the degree of CT, or ionicity, ρ in the three crystals. Sato *et al.*[11] used the $TCNQF_x$ bond lengths and the IR CN stretching frequency, obtaining somewhat contradictory inconsistent results, as shown in their Table S1. Both methods suffer in fact of some drawback: The bond lengths method depends on the adopted calibration, and the CN stretching frequency is known to give unreliable, generally overestimated, ρ values.[23] As in the case of perylene-$TCNQF_x$ series,[4] we have obtained ρ from the frequencies of other, well tested, IR active charge sensitive modes of $TCNQF_x$. [4,23,24]

Figure 3 reports the single crystal IR absorption spectra of BTBT-TCNQ, BTBT-$TCNQF_2$ and BTBT-$TCNQF_4$, collected with the electric field of the incident radiation perpendicular to the stack axis, so that the in-plane vibrational modes can be selectively observed. Only the spectral range 1350-1650 cm^{-1} is shown, since all the charge sensitive bands lie in this region. In Figure 3 we also report the spectra of BTBT powders, to show that bands originated by this molecule do not interfere with the identification of the charge sensitive bands of $TCNQF_x$ in the three co-crystals. Their frequency is reported directly in the Figure.

In the case of BTBT-TCNQ the ionicity is estimated through the position of the TCNQ $b_{1u}\nu_{20}$ C=C antisymmetric stretching. The frequency is shifted by 4 cm^{-1} with respect to the neutral TCNQ. Since the ionization frequency shift of this mode is 47 cm^{-1},[24] we obtain a ρ value of 0.10±0.02. For BTBT-$TCNQF_2$ two $TCNQF_2$ charge sensitive modes are identified at 1388 and 1569 cm^{-1}. In the neutral molecule they occur at 1393 and 1575 cm^{-1}, and have a ionization frequency shift of 44 and 50 cm^{-1}, respectively,[4] the resulting average ρ value is 0.11±0.03. BTBT-$TCNQF_4$ presents analogous charge sensitive modes at 1390 and 1590 cm^{-1}. Since in the neutral molecule they are observed at 1396 and 1599 cm^{-1}, with corresponding ionization frequency shift of 43 and 59 cm^{-1} respectively,[4,23] we obtain the average value $\rho = 0.14\pm0.03$.

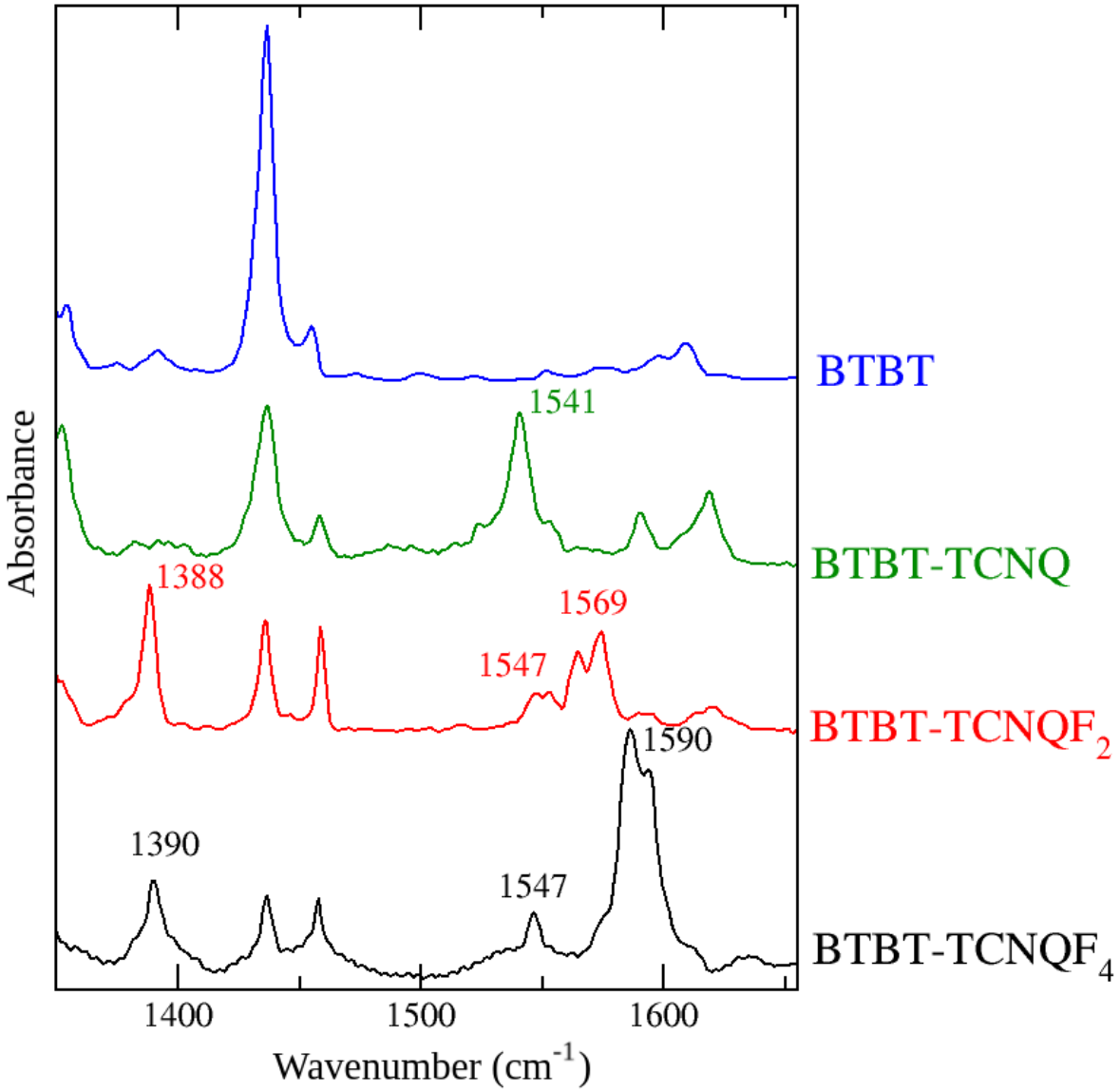

Figure 3. IR absorption spectra of BTBT-TCNQ (green line), BTBT-$TCNQF_2$ (red line), BTBT-$TCNQF_4$ (black line) single crystals, with polarization perpendicular to the stack axis. The top blue line is the spectrum of neutral BTBT powder. The frequencies of the charge sensitive bands are also reported.

The Raman spectra (see Supplementary Information) confirm that the degree of charge transfer remains more or less the same in the series, between 0.10 and 0.15. This is a somewhat surprising result, since combining the same donor with molecules of increasing electron affinity,

one would expect a increasing value of ρ, as it is the case for instance in series of perylene with $TCNQF_x$ or in the one involving 3,3',5,5'-tetramethylbenzidine with a wider series of electron acceptor molecules.[25]

DISCUSSION

Although infrequent, the relative insensitivity of the degree of CT to the difference between the ionization potential of the Donor and the electron affinity of the Acceptor has been already encountered. Besides the obviously similar case of the cocrystals $TCNQF_x$ with alkylated BTBT,[8,9] this unusual effect has been already explicitly noticed in the CT crystals formed from TCNQ and $TCNQF_4$ with dithieno[2,3-d;2',3'-d']benzo[1,2-b;4,5-b']dithiophene (DTBDT),[26] a molecule which presents some similarity with BTBT, being characterized by the same motif of two fused thiophene rings, separated by a benzene ring. In that case the authors used extensive DFT calculations to try to explain the phenomenon, ascribing it to a difference in the CT mechanism due to the presence of fluorine ligands.[26] We feel that such fully computational approach may be missing some relevant aspect, and in any case the proposed mechanism of the anomaly cannot be extended to the present case, where the overlap between Donor and Acceptor molecules is the same (Figure 2) in the three studied crystals, and where the BTBT-TCNQ and BTBT-$TCNQF_2$ crystals are isomorphous.

We have then decided to follow a different approach, where DFT calculations are only used to estimate the basic parameters entering a simplified Hamiltonian able to catch the essential physical-chemistry of mixed stack CT crystals. The method has been recently applied successfully to model a series of different CT crystals.[19] Since we are making a relative comparison in a series of similar molecules, we can safely assume that some of the relevant

parameters, like the intramolecular relaxation energy, is constant, so that we can limit the calculation to the following parameters: *t,* the hopping or CT integral between D and A; *V*, the DA intermolecular Coulomb potential; $z = (I_d - A_A) - (1/2)$ V, half the energy required to form an ionic pair[19] (I_d is the D ionization potential A_A the A electron affinity); and *M,* the Madelung energy.

Delchiaro *et al.*[19] used a CT dimer model to estimate *t* and *z*. However, this two-state model does not consider the possibility of having more than one CT integral, as it is known to occur in BTBT cocrystals: BTBT HOMO and HOMO-1 are close in energy (about 0.5 eV), so we have two CT integrals and two CT transitions.[8,9]

Table 2. Basic computed electronic parameters (eV) of the studied compounds

System	*z*	*t* [a]	*V*	*M*	*V - 2M*
BTBT-TCNQ	0.51	0.12, 0.23	- 2.12	- 0.96	-0.20
BTBT-$TCNQF_2$	0.25	0.09, 0.22	-2.06	-0.93	-0.20
BTBT-$TCNQF_4$	0.06	0.10, 0.22	-1.99	-0.99	-0.01
10BTBT-TCNQ	0.36	0.11, 0.21	-2.00	-1.00	0.00
	dimer: 0.76	dimer: 0.25			
10BTBT-$TCNQF_4$	-0.10	0.12, 0.21	-1.89	-0.95	0.02
	dimer: 0.57	dimer: 0.23			

[a] The two reported values of *t* correspond to the HOMO-LUMO and (HOMO-1)-LUMO integrals, in this order. In the case of 10BTBT-TCNQ and 10BTBT-$TCNQF_4$ the values obtained by the dimer model (Ref. 19) are reported for comparison.

In the present case we have therefore decided to directly calculate z and t. The latter corresponds to the Fock matrix elements between the involved D and A orthogonalized molecular orbitals.[21] The intermolecular Coulomb potential V and Madelung energy M are calculated in the point-charge approximation of the molecular charge density based on the computed atomic ESP charges. Finally, I_d and A_A energies entering (with V) in the definition of z are taken as the HOMO and LUMO DFT energies. The results of the calculations are summarized in Table 2.

Although only the *relative* value of the computed parameters is important here, we have nonetheless verified the effect of different choices in the DFT functional and basis set, taking as reference either the experimental values or the results from the dimer model.[19] The basis set choice has in general little influence, provided one uses an extended basis with diffuse contribution, as the 6-31G* of Gaussian[20] or the TZP of ADF.[21] The choice of functional instead affects considerably the orbital energies. In reporting z in Table 2, we use the ωB97XD MO energy values, shifting the zero of the energy in such a way that $(I_d - A_A)$ reproduces the experimental difference (1.57 eV) between the ionization potential of BTBT[27] and the TCNQ electron affinity.[28] In any case the difference between the two extremes, BTBT-TCNQ and BTBT-$TCNQF_4$ (about 0.5 eV) is essentially the same whatever DFT functional is adopted, and is always somewhat less than the difference between experimentally determined electron affinities of TCNQ and $TCNQF_4$.[28] In the calculation of t we can divide the effects of the functional in two categories: use of Generalized Gradient Approximations (GGA) always underestimates the t value, whereas hybrid methods such as B3LYP or ωB97XD overestimate it. In Table 2 we report the values obtained by GGA-PBE functional and TZP basis set, which compare well with those obtained with similar methods in Ref. [9], and which are underestimated

by a constant factor of 1.25 with respect to the experiment and to the dimer model.[19] Finally, the V and M values estimated form ESP charges do not depend significantly from the adopted functional and basis set.

In Table 2 we have added for comparison the electronic parameters of 2,7-didecyl[1]benzenothieno[3,2-b][1]benzothiophene (10BTBT) as calculated with the dimer model[19] and by the present method. It is seen that by increasing the TCNQ electron acceptor strength z, the energy required to form a DA pair (first column in Table 2) decreases, i.e., the system tend to become more ionic, as expected. The trend is confirmed by the computed degree of CT for the isolated DA pair in gas phase, ρ_{dim}:[19] it is close to zero for BTBT-TCNQ and increases by 0.02 in replacing TCNQ with $TCNQF_4$. It is indeed the Madelung energy which favors the more ionic state when the DA pair is embedded in the crystal, and it is the Madelung energy that makes the difference: It slightly decreases in going from BTBT-TCNQ to the isomorphous BTBT-$TCNQF_2$, then it increases in BTBT-$TCNQF_4$, despite the fact that in this case we have an increase of the volume per DA pair (Table 1). This nonlinear trend well explains the experimental values of the degree of charge transfer found in the three co-crystals: There is practically no change by replacing TCNQ with $TCNQF_2$, since the decrease of z is compensated by the decrease of M. In BTBT-$TCNQF_4$, on the other hand, both the decrease of z and the increase of M cooperate in shifting the system towards a more ionic state.

Even if both z and M contribute to increase the degree of CT in BTBT-$TCNQF_4$ with respect to BTBT-TCNQ, the increase is smaller than in other cases.[4] We believe that this is due to the effect of CT integral: The larger is t, the larger is the electron delocalization along the stack, and the smaller the effect of z and M.[19] In the case of BTBT we have two CT integrals, whose combined effect we believe is at the origin of the insensitivity of ρ to the increased electron affinity of the

$TCNQF_x$. Notice incidentally that the (HOMO-1)-LUMO CT integral is about twice the HOMO-LUMO one. This is due to a better overlap, as it can be appreciated from Figure 2. The fact that in BTBT the two frontier HOMOs are close in energy has been already remarked in the context of co-crystals involving BTBT and BTBT derivatives,[8,9] but as far as we know the consequences on the physical properties of the various systems have not been extensively addressed. For instance, the high hole mobility of alkyl-derivatives of BTBT[7] might be due to this fact.

We now try to understand why the Madelung energy slightly decreases in going from BTBT-TCNQ to the isomorphous BTBT-$TCNQF_2$, although the unit cell volume is decreasing (Table 1). As a matter of fact, the packing of the DA stacks explains the effect of the Madelung energy. This is clearly seen in Figure 4, which shows the layers of BTBT and $TCNQF_x$ perpendicular to the stacking axis of BTBT-TCNQ and BTBT-$TCNQF_2$. Since the structures have a DA pair per unit cell, the layers perpendicular to the stacks contains molecules of the same kind. Figure 4 reports the shortest distances between H, F and N atoms in nearby molecules. Since the (negative) molecular charge in $TCNQF_x$ is concentrated on the N, but also in F atoms when present, the repulsion between the stacks is increased in BTBT-$TCNQF_2$ with respect to BTBT-TCNQ, hence the decrease of the Madelung energy. This electrostatic effect may well explain why the BTBT-$TCNQF_4$ structure is not isomorphous with the other two. The presence of two more F atoms would make the triclinic structure less stable, with a further decrease of the electrostatic energy. Therefore BTBT-$TCNQF_4$ prefers to adopt the monoclinic structure, with two DA pairs per the unit cell, so that in the layers perpendicular to the stack we have the same kind of molecules along the *c* axis, but BTBT and $TCNQF_4$ alternate along the *a* axis (Figure S6).

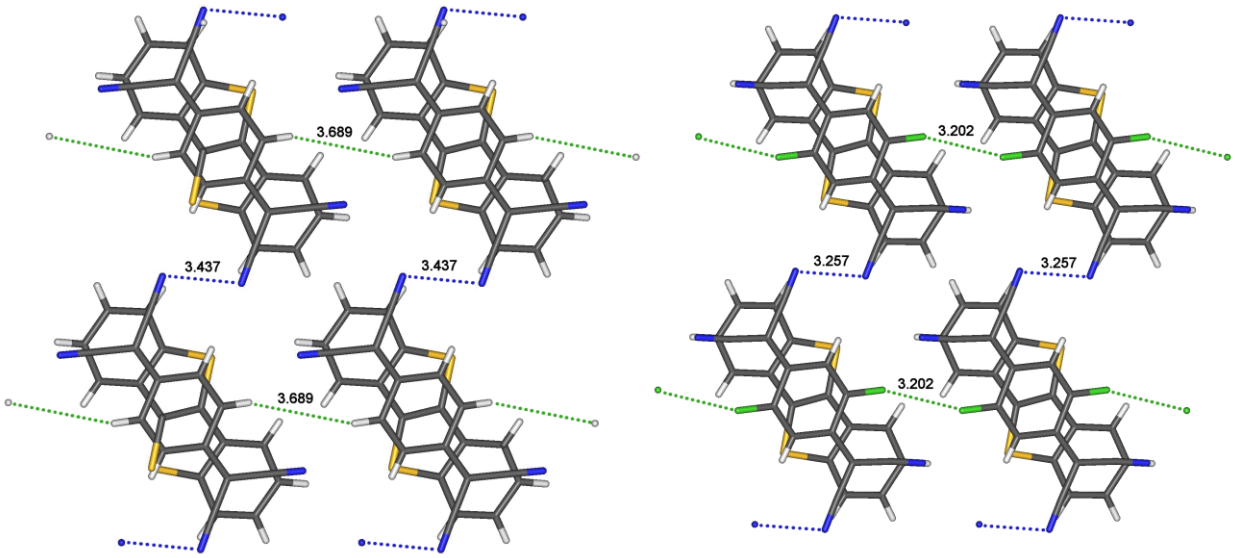

Figure 4. View of the isomorphous BTBT-TCNQ and BTBT-TCNQF$_2$ structures perpendicular to the stacking axis, showing the H-H, N-N and F-F shortest distances.

In order to give a more quantitative basis to the above discussion, we report in rightmost column of Table 2 the difference between V and $2M$ (the 2 factor is due to the definition of V and M). V represents the attractions between nearby oppositely charged molecules, and is essentially the intra-stack Coulomb potential. The Madelung energy M is instead the three-dimensional Coulomb potential, extended to the whole crystal and V - $2M$ is then representative of inter-stack interactions. Negative values, as in the case of BTBT-TCNQ and BTBT-TCNQF$_2$, point to the presence of dominant repulsive inter-stack interactions, larger than the attractive intra-stack interaction. A much larger negative value (-0.59) of $V - 2M$ is calculated for an hypothetical triclinic structure of BTBT-TCNQF$_4$, isomorphous with the other two structures in the series, confirming the idea that unfavorable electrostatic interactions are at the origin of the actual different three-dimensional packing. On the other hand, in systems with small or vanishing $V - 2M$, intra- and inter-stack interactions compensate each other. This is the case of BTBT-TCNQF$_4$, but also of 10BTBT-TCNQ and 10BTBT-TCNQF$_4$. The structure of the two latter systems is similar to that of BTBT-TCNQ, triclinic centro-symmetric with one DA pair per unit

cell, but in this case nearby equal molecules in the layer perpendicular to the stack are kept apart by the lateral alkyl chains.

CONCLUSIONS

In this paper we have presented a detailed structural and spectroscopic characterization of the series of CT crystals BTBT-TCNQF$_x$. At variance with other series involving different donors, like perylene,[4] the degree of CT appears to be rather insensitive to the TCNQF$_x$ electron accepting strength. Extensive calculations have allowed us to explain this finding in terms of the inter-stack packing of the co-crystals, and of the fact that both the HOMO and HOMO-1 of BTBT are involved in the CT mechanism. We underline that the small energy difference (~ 0.5 eV) between HOMO and HOMO-1 will have the likely consequence of the lack of symmetry between the conduction and valence band, a requirement for ambipolar transport in CT crystals.[1] Indeed, BTBT-TCNQF$_x$ co-crystals exhibit *n*-channel transport only.[11] On the other hand, this proximity might well explain the very good *p*-channel semiconducting properties of pristine BTBT derivatives.[7] In this paper we have also proposed to explain the difference in inter-stack packing resulting from increasing F substitution in TCNQ as due to the differences in electrostatic interactions. We believe this is an important clue in the endeavor to understand the role of weak interactions in the crystal packing of molecular crystals, and further studies in this direction are in progress in our laboratory.

ASSOCIATED CONTENT

Supporting Information.

The following files are available free of charge: Details on the X-ray structures, and relavant figures. Raman spectra of BTBT and of the co-crystals (PDF).

AUTHOR INFORMATION

Corresponding Author

*A. Girlando, Dipartimento di Scienze Chimiche, della Vita e della Sostenibilità Ambientale (SCVSA) and INSTM-UdR Parma, Università di Parma, Parco Area delle Scienze 17/a, IT-43124 Parma, Italy. E-mail: alberto.girlando@unipr.it

Author Contributions

The manuscript was written through contributions of all authors. All authors have given approval to the final version of the manuscript.

ACKNOWLEDGMENT

Parma University support to the research is acknowledged. The computational part has been supported by CINECA Consortium through Grant No. ISCRAC-HP10CAUAMPA.G. We also thank G. D'Avino (Institut Néel, Grenoble) for providing the MESCAL program and for assistance in its use. C.R. acknowledges the support of the MINECO of the Spanish Government (CTQ2016- 80030-R and SEV-2015-0496).

REFERENCES

(1) Zhu, L.; Yi, Y.; Li, Y.; Kim, E.-G.; Coropceanu, V.; Brédas, J.-L. *J. Am. Chem. Soc.* **2012**, *134* (4), 2340–2347.
(2) Salzmann, I.; Heimel, G.; Duhm, S.; Oehzelt, M.; Pingel, P.; George, B. M.; Schnegg, A.; Lips, K.; Blum, R.-P.; Vollmer, A.; Koch, N. *Phys. Rev. Lett.* **2012**, *108* (3).
(3) Hu, P.; Du, K.; Wei, F.; Jiang, H.; Kloc, C. *Cryst. Growth Des.* **2016**, *16* (5), 3019–3027.
(4) Salzillo, T.; Masino, M.; Kociok-Kohn, G.; Di Nuzzo, D.; Venuti, E.; Della Valle, R. G.; Vanossi, D.; Fontanesi, C.; Girlando, A.; Brillante, A.; Da Como, E. *Cryst. Growth Des.* **2016**, *16* (Copyright (C) 2016 American Chemical Society (ACS). All Rights Reserved.), 3028–3036.
(5) Morherr, A.; Witt, S.; Chernenkaya, A.; Bäcker, J.-P.; Schönhense, G.; Bolte, M.; Krellner, C. *Phys. B Condens. Matter* **2016**, *496*, 98–105.
(6) Yuan, Y.; Giri, G.; Ayzner, A. L.; Zoombelt, A. P.; Mannsfeld, S. C. B.; Chen, J.; Nordlund, D.; Toney, M. F.; Huang, J.; Bao, Z. *Nat. Commun.* **2014**, *5*, 3005.
(7) Tsutsui, Y.; Schweicher, G.; Chattopadhyay, B.; Sakurai, T.; Arlin, J.-B.; Ruzié, C.; Aliev, A.; Ciesielski, A.; Colella, S.; Kennedy, A. R.; Lemaur, V.; Olivier, Y.; Hadji, R.; Sanguinet, L.; Castet, F.; Osella, S.; Dudenko, D.; Beljonne, D.; Cornil, J.; Samorì, P.; Seki, S.; Geerts, Y. H. *Adv. Mater.* **2016**, *28* (33), 7106–7114.
(8) Méndez, H.; Heimel, G.; Opitz, A.; Sauer, K.; Barkowski, P.; Oehzelt, M.; Soeda, J.; Okamoto, T.; Takeya, J.; Arlin, J.-B.; Balandier, J.-Y.; Geerts, Y.; Koch, N.; Salzmann, I. *Angew. Chem. Int. Ed.* **2013**, *52* (30), 7751–7755.
(9) Tsutsumi, J.; Matsuoka, S.; Inoue, S.; Minemawari, H.; Yamada, T.; Hasegawa, T. *J Mater Chem C* **2015**, *3* (9), 1976–1981.
(10) Shibata, Y.; Tsutsumi, J.; Matsuoka, S.; Minemawari, H.; Arai, S.; Kumai, R.; Hasegawa, T. *Adv. Electron. Mater.* **2017**, 1700097.
(9) Sato, R.; Dogishi, M.; Higashino, T.; Kadoya, T.; Kawamoto, T.; Mori, T. J. Phys. Chem. C 2017, 121, 6561-6568.
(12) *APEX2, SAINT and SADABS*; Bruker AXS Inc.: Madison, Wisconsin, USA.
(13) Sheldrick, G. M. *Acta Crystallogr. Sect. Found. Adv.* **2015**, *71* (1), 3–8.
(14) Sheldrick, G. M. *Acta Crystallogr. Sect. C Struct. Chem.* **2015**, *71* (1), 3–8.
(15) Farrugia, L. J. *J. Appl. Crystallogr.* **2012**, *45* (4), 849–854.
(16) Keller, E. *SCHAKAL99, Graphical Representation of Molecular and Crystallographic Models*; University of Freiburg: Freiburg, Germany, 1999.
(17) *Jmol: an open-source Java viewer for chemical structures in 3D*.
(18) D'Avino, G.; Verstraete, M. J. *Phys. Rev. Lett.* **2014**, *113* (23).
(19) Delchiaro, F.; Girlando, A.; Painelli, A.; Bandyopadhyay, A.; Pati, S. K.; D'Avino, G. *Phys. Rev. B*.
(20) Frisch, M. J.; et al. *Gaussian 09*; Gaussian, Inc. Wallingford CT 2016, 2016.
(21) *ADF*; SCM, Theoretical Chemistry, Vrije Universiteit, Amsterdam, The Netherlands, http://www.scm.com.
(22) D'Avino, G.; Muccioli, L.; Zannoni, C.; Beljonne, D.; Soos, Z. G. *J. Chem. Theory Comput.* **2014**, *10* (11), 4959–4971.
(23) Meneghetti, M.; Pecile, C. *J. Chem. Phys.* **1986**, *84* (8), 4149–4162.
(24) Bozio, R.; Zanon, I.; Girlando, A.; Pecile, C. *J. Chem. Soc. Faraday Trans. 2* **1978**, *74*, 235.
(25) Masino, M.; Castagnetti, N.; Girlando, A. *Crystals* **2017**, *7* (4), 108.

(26) Chernenkaya, A.; Morherr, A.; Backes, S.; Popp, W.; Witt, S.; Kozina, X.; Nepijko, S. A.; Bolte, M.; Medjanik, K.; Öhrwall, G.; Krellner, C.; Baumgarten, M.; Elmers, H. J.; Schönhense, G.; Jeschke, H. O.; Valentí, R. *J. Chem. Phys.* **2016**, *145* (3), 034702.
(27) *Organic redox systems: synthesis, properties, and applications*; Nishinaga, T., Ed.; Wiley: Hoboken, New Jersey, 2016.
(28) Kanai, K.; Akaike, K.; Koyasu, K.; Sakai, K.; Nishi, T.; Kamizuru, Y.; Nishi, T.; Ouchi, Y.; Seki, K. *Appl. Phys. A* **2009**, *95* (1), 309–313.

SYNOPSIS